

REPORT 1210

ANALYSIS OF TURBULENT HEAT TRANSFER, MASS TRANSFER, AND FRICTION IN SMOOTH TUBES AT HIGH PRANDTL AND SCHMIDT NUMBERS¹

By ROBERT G. DEISSLER

SUMMARY

The expression for eddy diffusivity from a previous analysis was modified in order to account for the effect of kinematic viscosity on the turbulence in the region close to a wall. By using the modified expression, good agreement was obtained between predicted and experimental results for heat and mass transfer at Prandtl and Schmidt numbers between 0.5 and 3000. The effects of length-to-diameter ratio and of variable viscosity were also investigated for a wide range of Prandtl numbers.

INTRODUCTION

Most of the existing analyses for turbulent heat and mass transfer are adequate only for Prandtl and Schmidt numbers on the order of 1 or less. For instance, the analysis given in reference 1, although adequate for gases, gives heat- and mass-transfer coefficients for liquids at high Prandtl or Schmidt numbers that are higher than those obtained experimentally. The difference between the experimental values and the values obtained by the method in reference 1 increases as the Prandtl or Schmidt number increases. Coefficients obtained from the von Kármán analysis (ref. 2) at high Prandtl or Schmidt numbers are lower than the experimental values. Rannie's analysis (ref. 3) gives coefficients which are in somewhat better agreement with the data than either of these analyses, but the coefficients are again inaccurate at very high Prandtl or Schmidt numbers. The analysis of reference 4 agrees with data at Prandtl or Schmidt numbers of 1 and at very high Prandtl or Schmidt numbers, but the coefficients are somewhat low at intermediate values of these numbers. In reference 5, which was published since the present investigation was initiated, good agreement was obtained with mass-transfer data for Prandtl and Schmidt numbers between 0.5 and 3000 by introducing an appropriate amount of turbulence into the laminar sublayer. In all these analyses, except those in references 1 and 3, the properties were constant and the flow fully developed. The relations among heat transfer, mass transfer, and fluid friction are discussed in reference 6.

The inadequacy of most of the previous analyses at high Prandtl and Schmidt numbers is principally caused by the expressions used for the eddy diffusivity in the region very close to the wall. This region is important because of the extremely large temperature or concentration gradients in that region at high Prandtl or Schmidt numbers (ref. 7). In

the analysis given herein, which was made at the NACA Lewis laboratory, the expression for eddy diffusivity given in reference 1 is modified in order to account for the effect of kinematic viscosity in reducing the turbulence in the region close to the wall. The effects of variable viscosity and of length-to-diameter ratio are also investigated.

BASIC EQUATIONS

For obtaining the velocity, temperature, and concentration distributions in a tube with turbulent flow, the differential equations for shear stress, heat transfer, and mass transfer can be written as follows (symbols are defined in the appendix):

$$\tau = \mu \frac{du}{dy} + \rho \epsilon \frac{du}{dy} \quad (1)$$

$$q = -k \frac{dt}{dy} - \rho g c_p \epsilon_h \frac{dt}{dy} \quad (2)$$

$$m = -\lambda \frac{dC}{dy} - \epsilon_s \frac{dC}{dy} \quad (3)$$

where the values for ϵ and ϵ_h are dependent on the amount and kind of turbulent mixing at a point. The eddy diffusivities for heat and mass transfer are equal inasmuch as both processes are governed by the same differential equation if aerodynamic heating is neglected (diffusion equation). On the other hand, the ratio $\epsilon_h/\epsilon = \alpha$ must be determined experimentally or theoretically inasmuch as the equation of motion for a fluid contains terms which are not present in the diffusion equation. Equations (1) to (3) can be written in dimensionless form as

$$\frac{\tau}{\tau_0} = \left(\frac{\mu}{\mu_0} + \frac{\rho}{\rho_0} \frac{\epsilon}{\mu_0/\rho_0} \right) \frac{du^+}{dy^+} \quad (4)$$

$$\frac{q}{q_0} = \left(\frac{k}{k_0} \frac{1}{Pr_0} + \frac{\rho}{\rho_0} \frac{c_p}{c_{p,0}} \alpha \frac{\epsilon}{\mu_0/\rho_0} \right) \frac{dt^+}{dy^+} \quad (5)$$

$$\frac{m}{m_0} = \left(\frac{\lambda}{\lambda_0} \frac{1}{Sc_0} + \alpha \frac{\epsilon}{\mu_0/\rho_0} \right) \frac{dC^+}{dy^+} \quad (6)$$

The variation of properties in these equations might be caused by either radial variation of temperature or of concentration of the diffusing substance.

¹ Supersedes NACA TN 3145, "Analysis of Turbulent Heat Transfer, Mass Transfer, and Friction in Smooth Tubes at High Prandtl and Schmidt Numbers," by Robert G. Deissler, 1954.

EXPRESSIONS FOR EDDY DIFFUSIVITY

In order to make practical use of equations (4), (5), and (6), the eddy diffusivity ϵ must be evaluated for each portion of the flow. After consideration of the various factors on which ϵ might depend, the following functional relation is assumed:

$$\epsilon = \epsilon \left(u, y, \frac{\mu}{\rho}, \frac{du}{dy}, \frac{d^2u}{dy^2}, \dots \right) \quad (7)$$

(The quantities μ and ρ must occur together inasmuch as they are the only quantities in eq. (7) containing mass as a dimension.) It is assumed in reference 8 that in the region at a distance from the wall $\epsilon = \epsilon(du/dy, d^2u/dy^2)$ (Kármán's assumption), and in the region close to the wall $\epsilon = \epsilon(u, y) = n^2uy$. In both of these expressions the possible effect of kinematic viscosity μ/ρ is neglected. It appears from heat- and mass-transfer data at high Prandtl and Schmidt numbers, however, that the effect of μ/ρ cannot be neglected in the region very close to the wall ($y^+ < 5$). When the previous expressions are used to compute heat and mass transfer at high Prandtl and Schmidt numbers, the coefficients are considerably too high compared with the experimental values. It might be expected that, in the region very close to the wall where the turbulence level is low, the effect of kinematic viscosity would be important inasmuch as the viscous effects would be of the same order of magnitude as the inertia effects. Therefore, for the region close to the wall, ϵ is written as

$$\epsilon = \epsilon(u, y, \mu/\rho) \quad (8)$$

As in reference 8, the effect of the derivatives is neglected close to the wall because the flow is very nearly laminar in that region. The first derivative approaches the value u/y and hence may be omitted since u and y already appear in the functional relation. The second derivative becomes very nearly zero as the wall is approached.

From dimensional analysis, equation (8) becomes

$$\epsilon = n^2uyF\left(\frac{n^2uy}{\mu/\rho}\right) = \epsilon' F\left(\frac{\epsilon'}{\mu/\rho}\right) \quad (9)$$

The function $F[\epsilon'/(μ/ρ)]$ should approach 1 as ϵ or ϵ' increases, because the effect of kinematic viscosity becomes negligible at high turbulence levels. Inasmuch as dimensional analysis cannot determine the form of the function F , additional assumptions must be made.

The simplest assumption that might be made for $F[\epsilon'/(μ/ρ)]$ is that it equals $\epsilon'/(μ/ρ)$. This assumption could be written in differential form as

$$dF = d\left(\frac{\epsilon'}{\mu/\rho}\right) \quad (10)$$

However, equation (10) could not be expected to hold as F approaches 1, because the change in F for a given change in $\epsilon'/(μ/ρ)$ should approach 0 as F approaches 1 (F could never be greater than 1). The simplest multiplicative factor which gives equation (10) this characteristic is $(1-F)$. The assumption made for the variation of F , the adequacy of which will be checked by experiment, therefore becomes

$$dF = d[\epsilon'/(μ/ρ)](1-F) \quad (11)$$

Separating variables and integrating from the wall to a point in the fluid give

$$\int_0^F \frac{dF}{1-F} = \int_0^{\epsilon'/(μ/ρ)} d\left(\frac{\epsilon'}{\mu/\rho}\right) \quad (12)$$

where the lower limits are taken as zero, because the turbulence goes to zero at the wall and the effect of kinematic viscosity consequently becomes extremely large at the wall ($F \rightarrow 0$). Integration of equation (12) results in

$$F = 1 - e^{-\frac{\epsilon'}{\mu/\rho}} \quad (13)$$

This expression approaches 1 for large values of $\epsilon'/(μ/ρ)$. From equations (9) and (13) there results

$$\epsilon = n^2uy \left(1 - e^{-\frac{n^2uy}{\mu/\rho}}\right) \quad (14)$$

Equation (14) gives ϵ as a function of u and y for the region close to the wall. The constant n is to be determined experimentally.

For the region at a distance from the wall, F is usually close to 1, because the effect of kinematic viscosity is small. The Kármán expression for ϵ , which neglects the variation of F , can usually be used in that region, or

$$\epsilon = \kappa^2 \frac{(du/dy)^3}{(d^2u/dy^2)^2} \quad (15)$$

If it is desired to take the variation of F into account in the region at a distance from the wall, equation (15) becomes

$$\epsilon = \kappa^2 \frac{(du/dy)^3}{(d^2u/dy^2)^2} \left[1 - e^{-\frac{\kappa^2 (du/dy)^3 / (d^2u/dy^2)^2}{\mu/\rho}}\right] \quad (16)$$

No attempt is made in the present analysis to specify the mechanism by which the kinematic viscosity reduces the eddy diffusivity in the region close to the wall, because the exact mechanism is unknown. Possible mechanisms are these: First, the kinematic viscosity might act as a damping factor to reduce the turbulence level close to the wall. Second, it might help to orient the eddies close to the wall by damping out those moving perpendicular to the wall and thus reduce the effective turbulent transfer. Third, it might act to produce a partial turbulence; that is, it might cause the flow at a point to be laminar a fraction of the time. The actual effect of kinematic viscosity might be due to any, or all, of these mechanisms.

ANALYSIS FOR CONSTANT FLUID PROPERTIES

In order to solve equations (4), (5), and (6), the following assumptions are made in addition to the assumptions concerning the expressions for eddy diffusivity (eqs. (14), (15), and (16)):

(1) The eddy diffusivities for momentum ϵ and heat or mass transfer ϵ_h are equal, or $\alpha = 1$. Previous analyses for flow of gases in tubes based on this assumption yielded heat-transfer coefficients that agree with experiment (ref. 1). At low Peclet numbers ($Pe = RePr$), α appears to be a function

of Peclet number (ref. 9) but is approximately 1 at high Peclet numbers. In general, the Peclet numbers are high at high Prandtl numbers for turbulent flow.

(2) The variations across the tube or boundary layers of shear stress τ , the heat transfer per unit area q , and the mass transfer per unit area m have a negligible effect on the velocity, temperature, and concentration distributions. It is shown in figure 12 of reference 1 that the assumption of a linear variation of shear stress and heat transfer across the boundary layers gives very nearly the same velocity and temperature profiles for gases as those obtained by assuming uniform shear stress and heat transfer across the boundary layers for values of δ_h^+ between 500 and 5000. (The boundary layers fill the tube for fully developed flow or fully developed heat or mass transfer.) For small values of δ_h^+ , such as occur very near the entrance, the effect of variable heat transfer (or mass transfer) is checked in figure 9 of reference 10 and found to be negligible. Although these checks were made for gases (Prandtl or Schmidt numbers close to 1), the effect of variation of heat or mass transfer per unit area at high Prandtl or Schmidt numbers would be even less because the temperature or concentration profile becomes flatter as the Prandtl or Schmidt number is increased.

(3) The molecular shear-stress, heat-transfer, and mass-transfer terms in the equations can be neglected in the region at a distance from the wall (ref. 1, fig. 14).

(4) In the case of mass transfer, the concentration of the diffusing substance is small enough that the mass transfer does not appreciably change the velocity. This condition

is generally obtained in the case of evaporation from a wetted wall or in the solution of the wall material in a liquid.

Velocity, temperature, and concentration distributions.—The expression for ϵ close to the wall (eq. (14)) can be written in dimensionless form for constant properties as

$$\frac{\epsilon}{\mu_0/\rho_0} = n^2 u^+ y^+ (1 - e^{-n^2 u^+ y^+}) \quad (17)$$

Equations (4), (5), and (6) can be written in integral form for the region close to the wall with the preceding assumptions and constant fluid properties as

$$u^+ = \int_0^{y^+} \frac{dy^+}{1 + n^2 u^+ y^+ (1 - e^{-n^2 u^+ y^+})} \quad (18)$$

$$t^+ = \int_0^{y^+} \frac{dy^+}{\frac{1}{Pr} + n^2 u^+ y^+ (1 - e^{-n^2 u^+ y^+})} \quad (19)$$

$$G^+ = \int_0^{y^+} \frac{dy^+}{\frac{1}{Sc} + n^2 u^+ y^+ (1 - e^{-n^2 u^+ y^+})} \quad (20)$$

For the region at a distance from the wall, equation (15) is substituted in equations (4), (5), and (6). By use of assumptions (2) and (3), equation (4) becomes, for constant fluid properties,

$$u^+ - u_1^+ = \frac{1}{\kappa} \log_e \left(\frac{y^+}{y_1^+} \right) \quad (21)$$

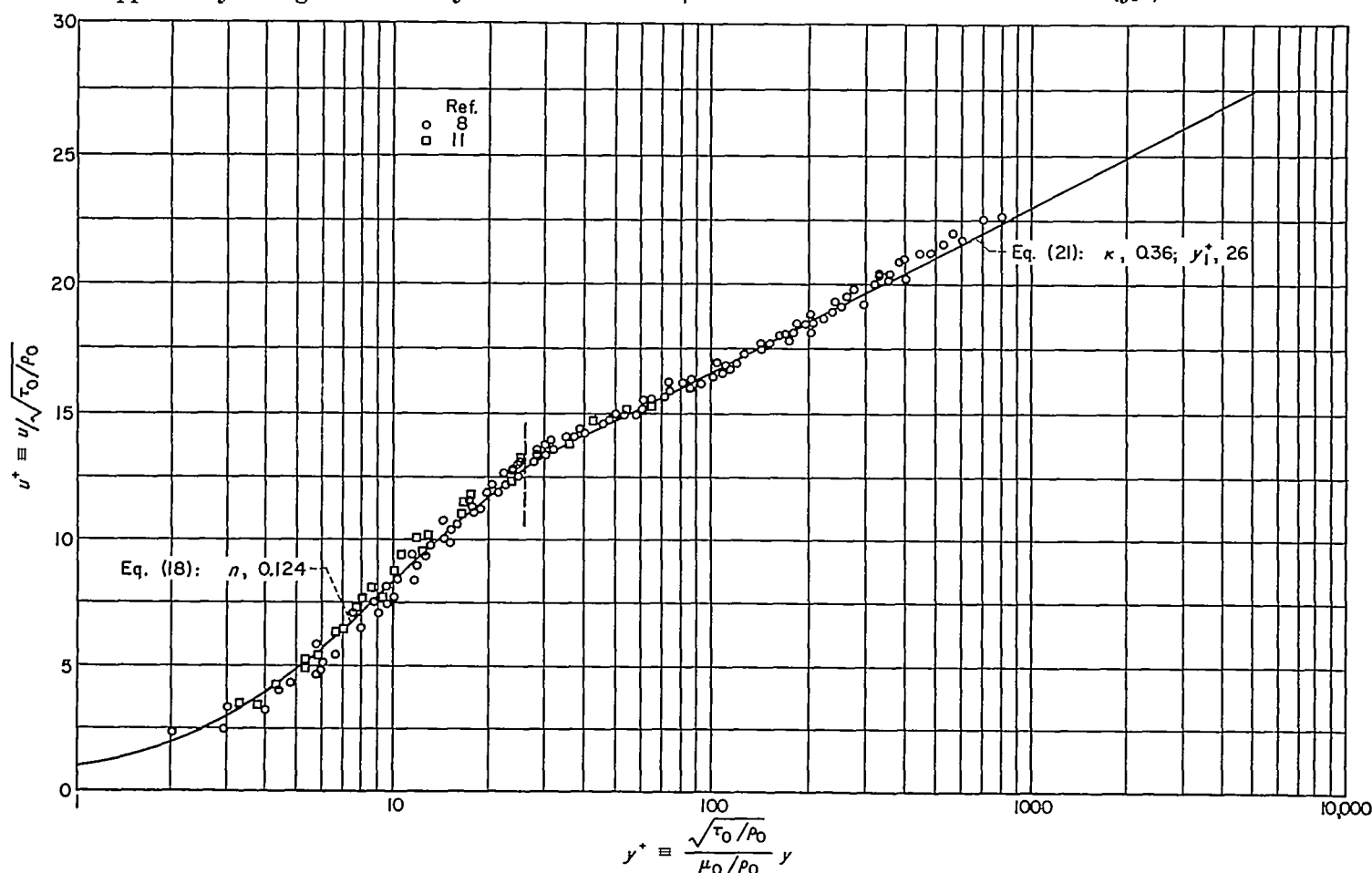


FIGURE 1.—Generalized velocity distribution for adiabatic turbulent flow. (Vertical line is dividing line between eqs.)

which is the well-known logarithmic equation. Division of equation (4) by equation (5) or (6) gives, with assumptions (1), (2) and (3),

$$u^+ - u_1^+ = t^+ - t_1^+ = C^+ - C_1^+ \quad (22)$$

where the equations are integrated from y_1^+ , the lowest value of y^+ for which the equations for flow at a distance from the wall apply, to y^+ .

The variation of u^+ with y^+ for fully developed adiabatic turbulent flow from references 8 and 11 is shown on semi-logarithmic coordinates in figure 1. The curves corresponding to equations (18) and (21) are also shown in the figure. Equation (18) was solved by numerical iteration inasmuch as u^+ occurs on both sides of the equation. The values of the constants in the equations are $n=0.124$, $\kappa=0.36$, and $y_1^+=26$, as determined from the experimental data. These values will apply also to the temperature distributions. The value of n in equation (18) differs from that given in reference 8 because equation (18) includes the effect of kinematic viscosity on ϵ . Figure 1 indicates good agreement of equation (18) with the data for $y^+ < 26$ and of equation (21) with the data for $y^+ > 26$. From the velocity-distribution data it is difficult to tell whether $\epsilon = n^2 u y$ from reference 8 or equation (14) for ϵ should be used in the region close to the wall, inasmuch as both expressions give results which agree closely with the data. The temperature or concentration profiles at high Prandtl or Schmidt numbers are, however, much more sensitive to the values of ϵ very close to the wall because of the very large temperature or concentration gradients in that region, as can be seen in figure 2.

Generalized temperature or concentration distributions calculated from equations (19), (20), and (22) are presented in figure 2 on log-log coordinates. Each curve represents either t^+ or C^+ at a given Prandtl or Schmidt number, as can be seen by comparison of equations (19) and (20). The curves indicate that the temperature or concentration distributions become flatter over most of the tube radius as the Prandtl or Schmidt number increases. From equations (19) and (20), $dt^+/dy^+ = Pr$ and $dC^+/dy^+ = Sc$ at or very near the wall so that the slopes of the curves at the wall increase with Prandtl or Schmidt number. The slopes of the curves in figure 2 near the wall appear equal because the curves are plotted on log-log coordinates ($d(\log t^+)/d(\log y^+) = 1$ at the wall). Included for comparison is the temperature distribution for a Prandtl number of 300 calculated by the method in reference 1, which neglects the effect of kinematic viscosity ($\epsilon = n^2 u y$).

The sensitivity of the temperature or concentration distribution at high Prandtl or Schmidt numbers to various assumptions for the turbulent transfer in the region close to the wall compared with that of the velocity distribution indicates that the region very close to the wall could be studied advantageously by measuring temperatures or concentrations at high Prandtl or Schmidt numbers rather than by measuring velocities in that region. Some work along these lines has been reported in reference 5, in which concentration profiles at high Schmidt numbers were measured with an interferometer. No evidence of a purely laminar layer (linear concentration profile) was found for values of

y^+ as low as 1. This result is in agreement with the assumption in the present analysis, where the turbulence is assumed to be zero only at the wall.

Relations among Nusselt, Reynolds, and Prandtl or Schmidt numbers for constant properties.—It can be shown from the definitions of the quantities involved that the Nusselt numbers for heat and mass transfer and the Reynolds number are given by

$$Nu = \frac{2r_0^+ Pr}{t_b^+} \quad (23)$$

$$Nu' = \frac{2r_0^+ Sc}{C_b^+} \quad (24)$$

$$Re = 2u_b^+ r_0^+ \quad (25)$$

where

$$t_b^+ = \frac{\int_0^{r_0^+} t^+ u^+ (r_0^+ - y^+) dy^+}{\int_0^{r_0^+} u^+ (r_0^+ - y^+) dy^+} \quad (26)$$

$$C_b^+ = \frac{\int_0^{r_0^+} C^+ u^+ (r_0^+ - y^+) dy^+}{\int_0^{r_0^+} u^+ (r_0^+ - y^+) dy^+} \quad (27)$$

and

$$u_b^+ = \frac{2}{(r_0^+)^2} \int_0^{r_0^+} u^+ (r_0^+ - y^+) dy^+ \quad (28)$$

The Nusselt numbers in these equations are based on the difference between wall and bulk temperatures or concentrations. The relation among Nusselt, Reynolds, and Prandtl numbers can be obtained from these equations and the generalized distributions given in figures 1 and 2 for various values of the parameter r_0^+ .

Predicted Nusselt numbers for fully developed heat or mass transfer are plotted against Reynolds number for various

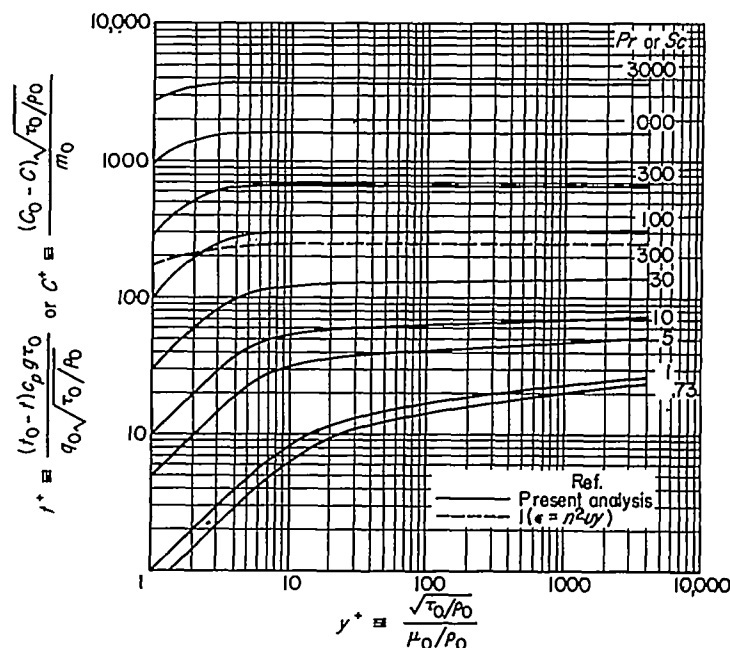


FIGURE 2.—Generalized temperature or concentration distributions for various Prandtl or Schmidt numbers.

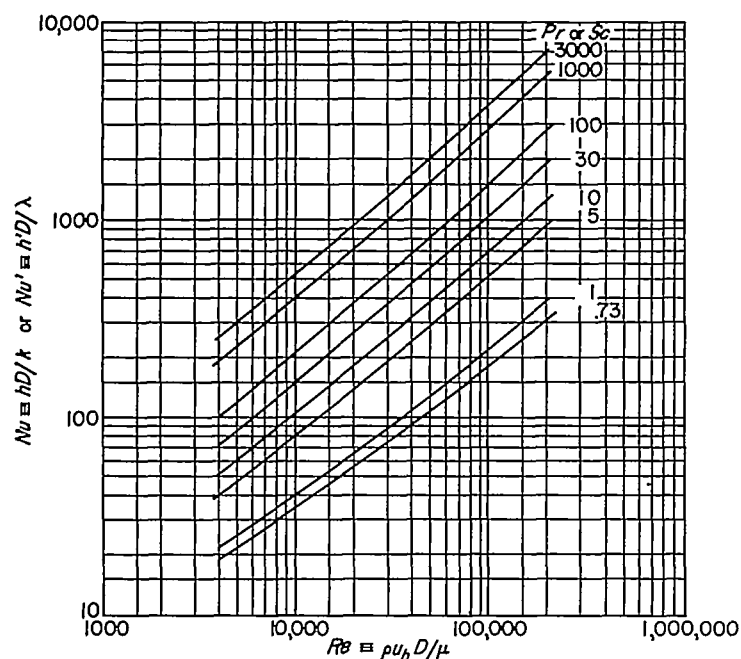


FIGURE 3.—Fully developed Nusselt numbers for heat or mass transfer against Reynolds number for various Prandtl or Schmidt numbers.

values of Prandtl or Schmidt number in figure 3. The curve for a Prandtl number of 0.73 agrees very closely with that given in reference 1, which was obtained by using $\epsilon = n^2 u y$ in the region close to the wall. The curves for supercritical water at higher Prandtl numbers ($Pr \approx 6$) given in references 12 (fig. 7) and 13 (fig. 18), however, are higher than those in figure 3; therefore the curves in these references should be replaced by figure 3, although the values of the reference temperatures for evaluating the fluid properties should not be significantly affected.

Examination of the curves in figure 3 indicates that the slopes of the various curves are approximately equal on a log-log plot. (The slopes would be more nearly equal if the Peclet number effect from ref. 9 were included.) This result justifies the usual practice in heat-transfer investigations of writing $Nu = f(Re, Pr)$ as $f(Re) \times f(Pr)$ (usually as $Re^a Pr^b$). The same result does not hold for very low Prandtl numbers where the slopes change considerably.

Comparison of analysis and experiment for fully developed heat and mass transfer.—A comparison between predicted and experimental results for fully developed heat and mass transfer is presented in figure 4, in which Stanton number is plotted against Prandtl or Schmidt number for various Reynolds numbers. The predicted Stanton numbers were obtained from figure 3 and the relation $St = Nu/RePr$. The symbols represent mean lines through data for heat transfer in gases (ref. 1) and in liquids (refs. 14 to 19) and mass transfer by evaporation from wetted walls (refs. 20 to 22), by solution of the wall material in a liquid (refs. 23 and 24), and by diffusion-controlled electrodes (ref. 25). The predicted and measured values are in good agreement over the entire range of Prandtl and Schmidt numbers shown (0.5 to 3000). The agreement for a Reynolds number of 10,000 in the low Prandtl or Schmidt number range would be improved by applying the Peclet number correction from reference 9.

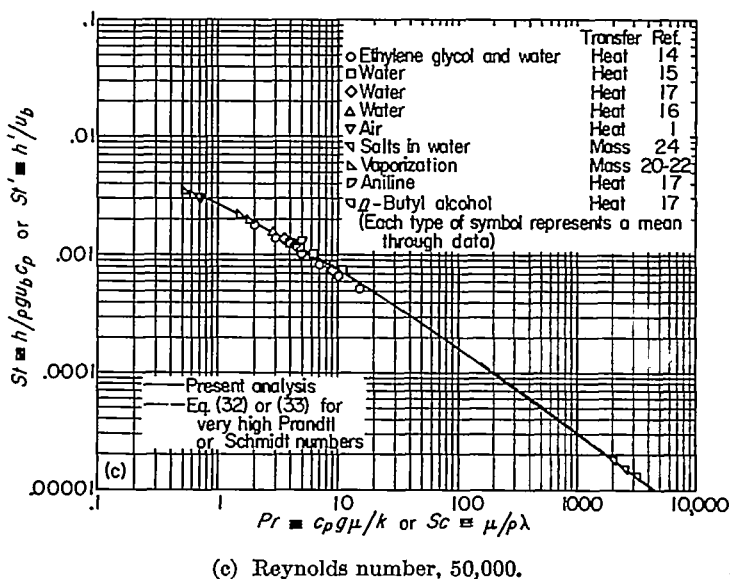
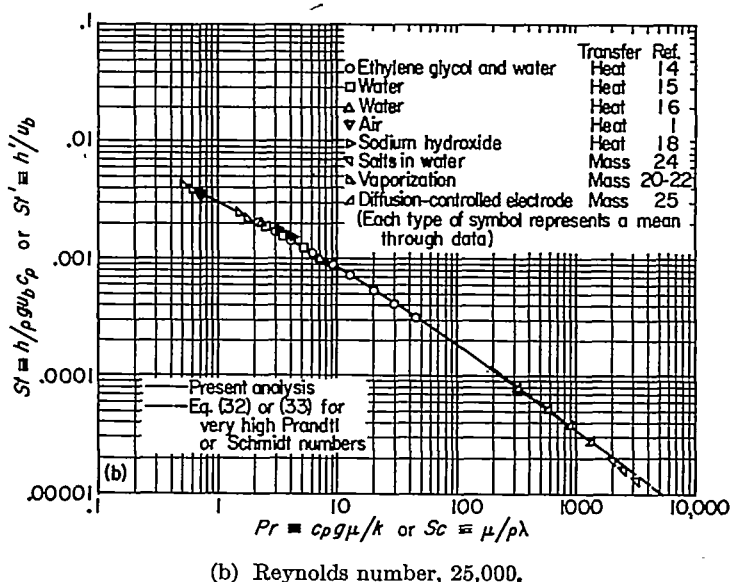
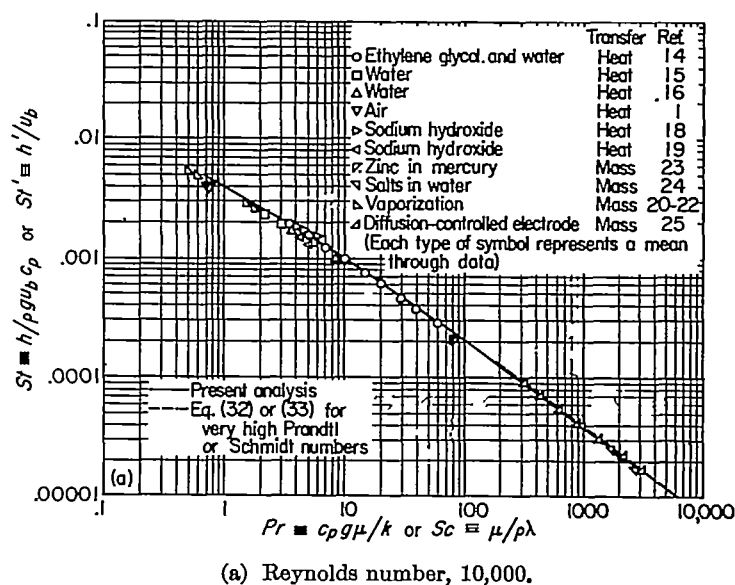


FIGURE 4.—Comparison of analytical and experimental results for fully developed heat and mass transfer.

Simplified equation for fully developed case for very high Prandtl or Schmidt numbers.—At very high Prandtl numbers the essential temperature changes take place in the region very close to the wall where u^+ is very nearly equal to y^+ . Setting $u^+=y^+$ in equation (19), expanding the exponential function in a series, and retaining only the first two terms of the series result in

$$t^+ = \int_0^{y^+} \frac{dy^+}{\frac{1}{Pr} + n^4(y^+)^4} \quad (29)$$

Integration of equation (29) and evaluation of the result for $y^+=\infty$ give

$$t_b^+ = \frac{\pi}{2\sqrt{2}n} Pr^{3/4} \quad (30)$$

The value of t^+ at $y^+=\infty$ is essentially t_b^+ , because t^+ is very nearly constant except in the region very close to the wall at high Prandtl numbers. From equations (23) and (30),

$$Nu = \frac{4\sqrt{2}}{\pi} n r_0^+ Pr^{1/4} \quad (31)$$

or the Stanton number, in terms of the Prandtl number and friction factor, is

$$St = \frac{2n}{\pi} \frac{\sqrt{f}}{Pr^{3/4}} \quad (32)$$

where

$$f = \frac{2}{(u_b^+)^2}$$

Similarly, for mass transfer,

$$St' = \frac{2n}{\pi} \frac{\sqrt{f}}{Sc^{3/4}} \quad (33)$$

where n has the value 0.124 as determined in figure 1. The relation between Re and f is given in figure 8 of reference 1 or the curve in figure 10 in the present report for adiabatic flow ($\beta=0$). This relation is, of course, independent of Prandtl number for constant properties. Equation (32) or (33) is indicated by the dotted line in figure 4 and is seen to be in good agreement with the predicted line obtained previously for $Pr > 200$.

Comparison of various analyses.—A comparison of various analyses is given in figure 5. It can be seen that all the analyses more or less converge at the lower Prandtl or Schmidt numbers. At the high Prandtl or Schmidt numbers, the present analysis and the analyses from references 4 and 5 are in fair agreement, whereas those from references 2 and 3 diverge considerably. The present analysis and the analysis from reference 5 represent the experimental data about equally well.

Heat or mass transfer in entrance region for uniform wall heat or mass flux, uniform initial temperature or concentration distribution, fully developed velocity distribution, and constant properties.—For calculating heat or mass transfer in the entrance region, it is assumed, as in reference 10, that the effects of heat or mass transfer are confined to fluid layers close to the surface (boundary layers for heat or mass transfer). The temperature or concentration distributions outside the boundary layers are assumed uniform, and the

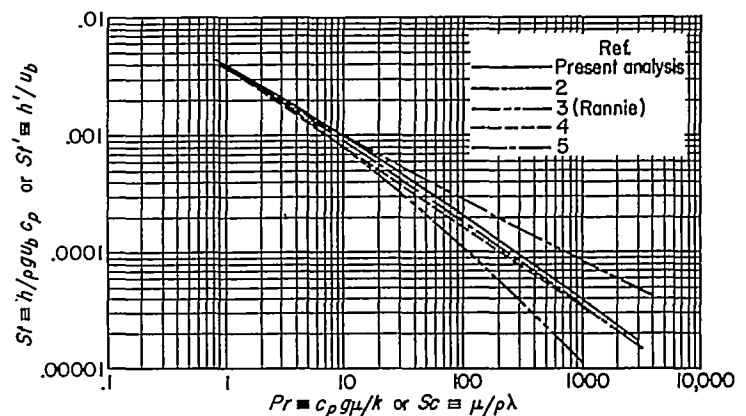


FIGURE 5.—Comparison of various analyses. Reynolds number, 10,000.

temperature or concentration is constant along the length of the tube for the region outside the boundary layer. Inside the boundary layer the temperature or concentration distribution is obtained from figure 2. Integral heat- or mass-transfer equations are used for calculating the thickness of the boundary layers for various distances from the entrance. It is shown in reference 10 that for heat transfer the relation between δ_h^+ and X/D for constant properties is given by

$$\frac{X}{D} = \frac{1}{2(r_0^+)^2} \int_0^{\delta_h^+} (t_b^+ - t^+) u^+(r_0^+ - y^+) dy^+ \quad (34)$$

A similar equation can be written for mass transfer if the concentration of the diffusing material is small (assumption 4):

$$\frac{X}{D} = \frac{1}{2(r_0^+)^2} \int_0^{\delta_h^+} (C_b^+ - C^+) u^+(r_0^+ - y^+) dy^+ \quad (35)$$

In equations (34) and (35), X represents the axial distance from the point at which heat or mass transfer begins. The dimensionless boundary-layer thickness δ_h^+ is the same in both equations when the Prandtl number equals the Schmidt number inasmuch as $C^+=t^+$ for a given value of y^+ and Prandtl or Schmidt number.

Values of local Nusselt and Reynolds numbers can be obtained from equations (23), (24), and (25), as for fully developed flow, with the exception that the expression for t_b^+ in equation (26) is replaced by

$$t_b^+ = \frac{\int_0^{\delta_h^+} t^+ u^+(r_0^+ - y^+) dy^+ + t_b^+ \int_{\delta_h^+}^{r_0^+} u^+(r_0^+ - y^+) dy^+}{\int_0^{r_0^+} u^+(r_0^+ - y^+) dy^+} \quad (36)$$

A similar expression can be obtained for C_b^+ . The integral in the numerator is broken into two parts, because t^+ is constant and equal to t_b^+ outside the thermal boundary layer. Inside the thermal boundary layer the relation between t^+ and y^+ is obtained from figure 2. Values of u^+ are obtained from figure 1 for y^+ from 0 to r_0^+ inasmuch as a fully developed velocity distribution is assumed. The relation between Nusselt number and X/D for various values of Reynolds number is obtained by assuming values of the parameters r_0^+ and δ_h^+ and by calculating the various quantities from equations (23), (25), (34), and (36).

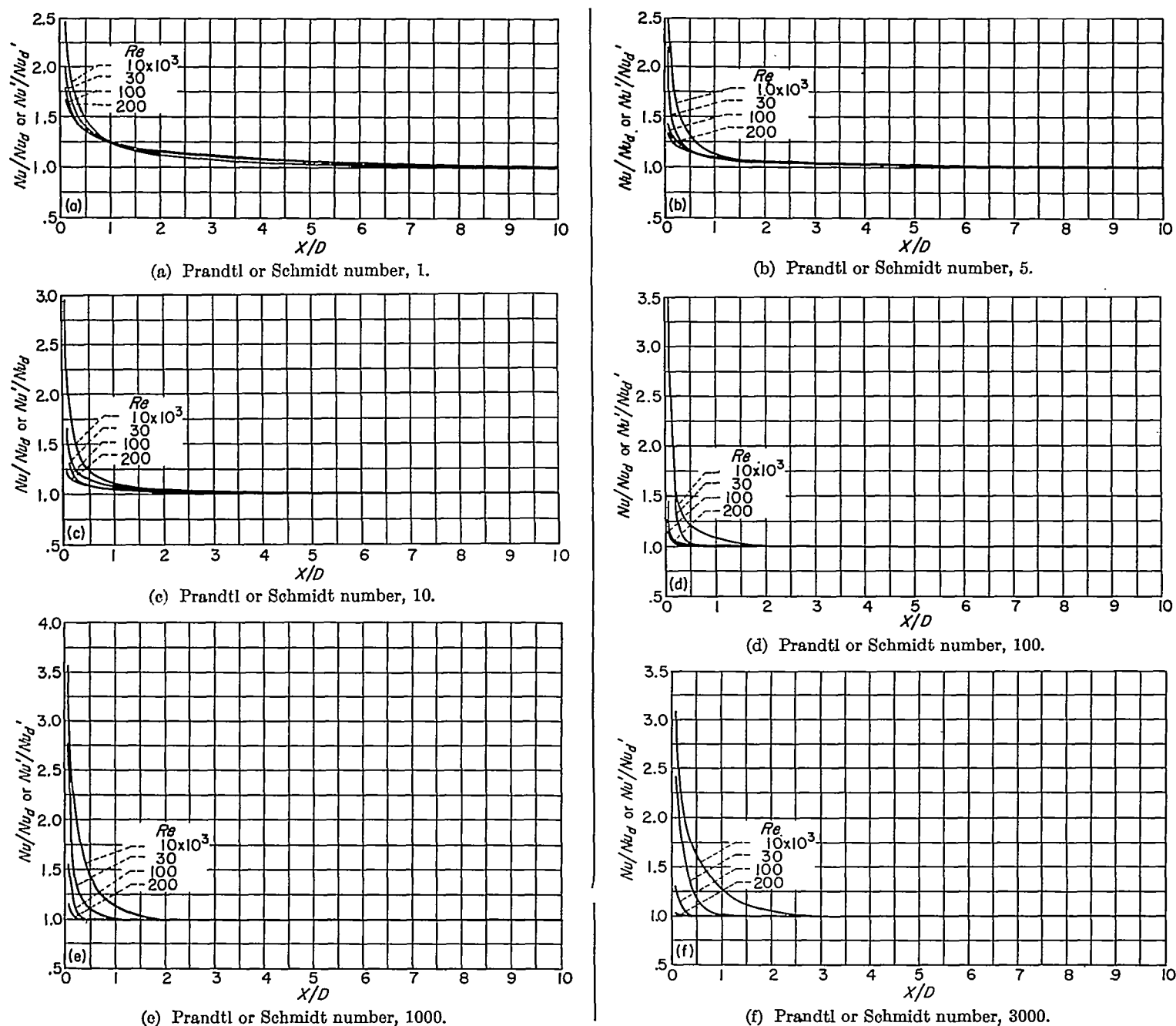


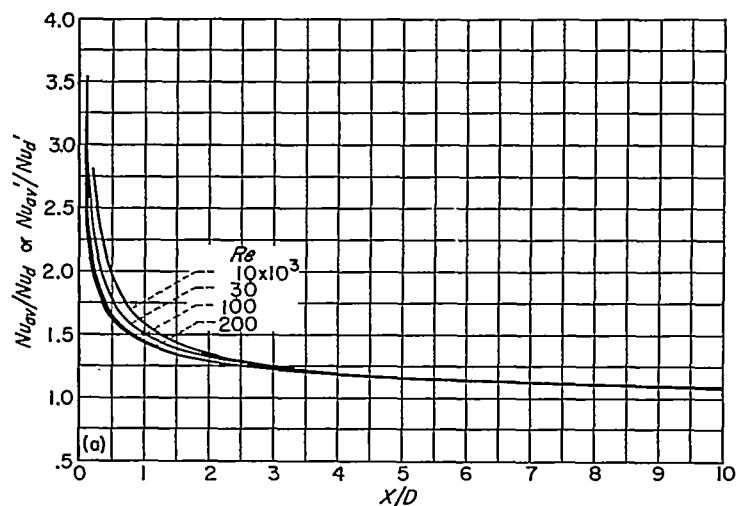
FIGURE 6.—Variation of local Nusselt number over fully developed Nusselt number for heat or mass transfer with X/D and Reynolds number. Uniform wall heat flux, uniform initial temperature distribution, and fully developed velocity distribution.

The variation of local Nusselt number for heat or mass transfer divided by the fully developed Nusselt number with X/D and Reynolds number at Prandtl or Schmidt numbers between 1 and 3000 is given in figure 6. At the higher Reynolds numbers the values of Nu/Nu_d for a given X/D decrease with increasing Prandtl number; that is, the effect of X/D becomes small at large values of Prandtl number. At low Reynolds numbers the variation is more complex: Values of Nu/Nu_d first decrease and then increase slightly as Prandtl number increases. In either case it is evident that in the entrance region the fully developed Nusselt numbers should be multiplied by a factor which is a function of X/D , Reynolds number, and Prandtl number rather than of X/D alone. That is, a simple factor such as $(X/D)^{-c}$,

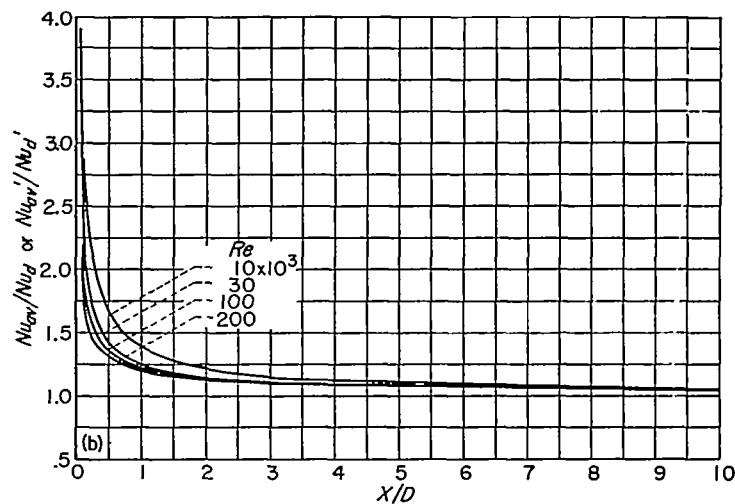
which is often used for Prandtl numbers of approximately 1, is inadequate for high Prandtl numbers. The effect of Reynolds number on Nusselt number in the entrance region increases with Prandtl number; that is, the separation of the curves for various Reynolds numbers increases. The same conclusions apply to the average Nusselt numbers plotted in figure 7 except that the changes with X/D near the entrance are more gradual and the separation of the curves with Reynolds number is greater than for the local values.

The average Nusselt numbers were calculated from

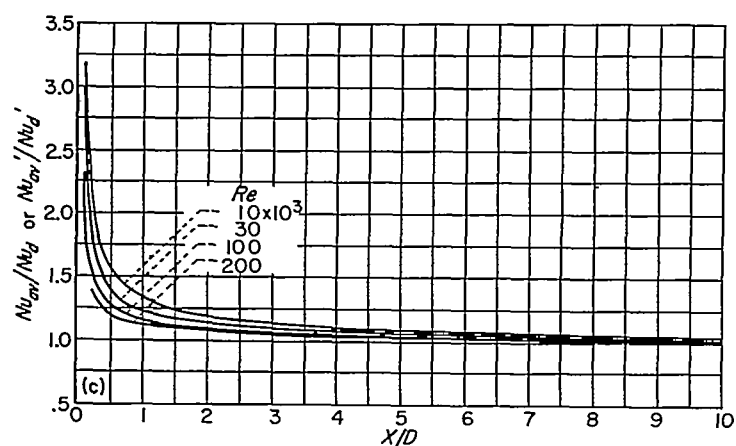
$$Nu_{av} = \frac{X/D}{\int_0^{X/D} \frac{d(X/D)}{Nu}}$$



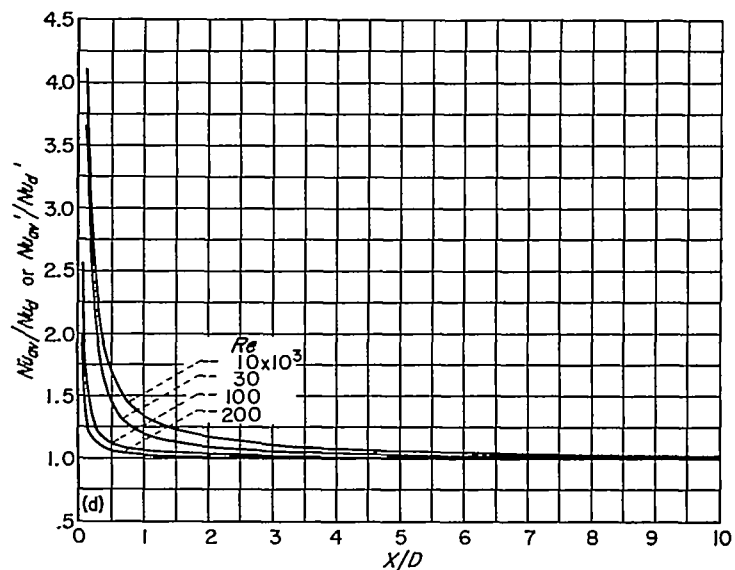
(a) Prandtl or Schmidt number, 1.



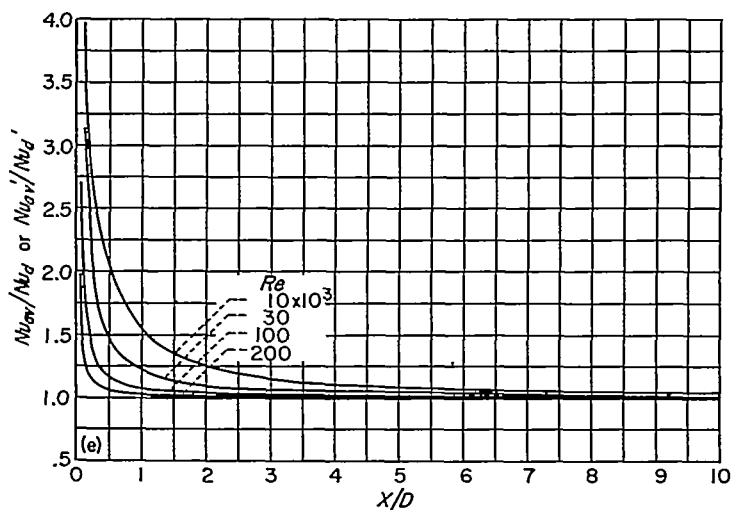
(b) Prandtl or Schmidt number, 5.



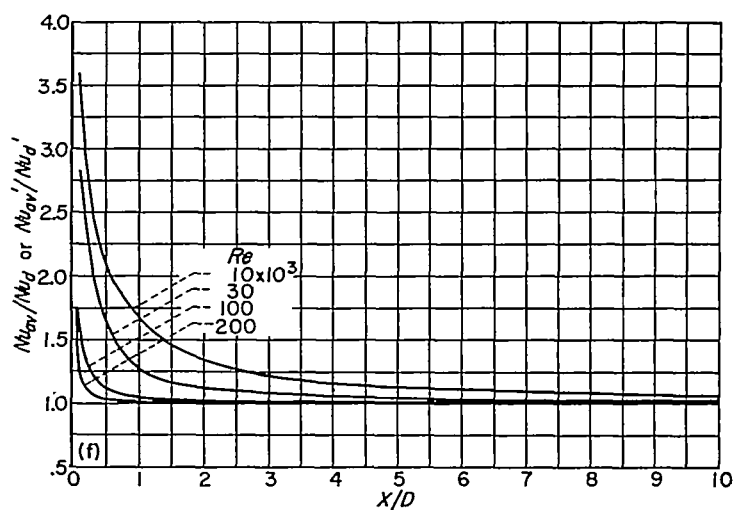
(c) Prandtl or Schmidt number, 10.



(d) Prandtl or Schmidt number, 100.



(e) Prandtl or Schmidt number, 1000.



(f) Prandtl or Schmidt number, 3000.

FIGURE 7.—Variation of average Nusselt number over fully developed Nusselt number for heat or mass transfer with X/D and Reynolds number. Uniform wall heat flux, uniform initial temperature distribution, and fully developed velocity distribution.

This equation is consistent with the definition

$$(t_0 - t_b)_{av} = \frac{\int_0^X (t_0 - t_b) dX}{X}$$

which is the usual way of defining the average difference between wall and bulk temperatures for uniform heat flux.

It is of interest to note that the Nusselt numbers for turbulent flow in figures 6 and 7, in general, display trends opposite to those for Nusselt numbers for laminar flow with increasing values of Prandtl number. In the case of laminar flow, the value of Nu/Nu_d at a given X/D and Reynolds number increases considerably with Prandtl number (ref. 26, fig. 3), because the heat diffuses through the fluid more slowly at the higher Prandtl numbers (the thermal diffusivity is lower) so that the thermal boundary layer is thinner and Nu/Nu_d for a given X/D near the entrance and a given Reynolds number is consequently higher than for the lower Prandtl numbers. The same phenomenon also tends to increase the effect of X/D for turbulent heat transfer. In the case of turbulent heat transfer, however, the shape of the temperature profile in the thermal boundary layer changes considerably with Prandtl number and becomes very flat at high Prandtl numbers (fig. 2). This means that the temperature profiles for fully developed flow do not differ greatly from those near the entrance (both are flat) although the boundary-layer thickness for the two cases differs considerably. The Nusselt numbers in the entrance region for turbulent heat transfer at high Prandtl numbers therefore tend to quickly approach the fully developed values.

FULLY DEVELOPED HEAT TRANSFER AND FRICTION WITH VARIABLE PROPERTIES

Turbulent heat transfer to liquids with variable viscosity.—In the case of heat transfer to liquids, the variation of the viscosity with temperature is considerably greater than the variation of the other properties. A good approximation to the actual heat transfer in liquids can therefore be obtained by considering only the viscosity to vary with temperature. Under that assumption and assumptions 1 and 2 from the section ANALYSIS FOR CONSTANT FLUID PROPERTIES, equations (4) and (5) become

$$1 = \left(\frac{\mu}{\mu_0} + \frac{\epsilon}{\mu_0/\rho_0} \right) \frac{du^+}{dy^+} \quad (37)$$

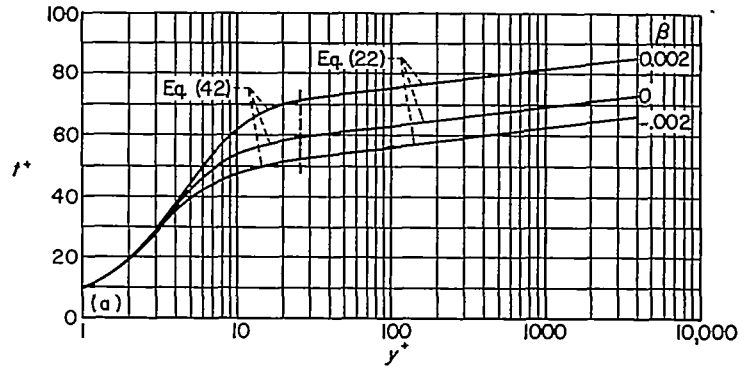
and

$$1 = \left(\frac{1}{Pr_0} + \frac{\epsilon}{\mu_0/\rho_0} \right) \frac{dt^+}{dy^+} \quad (38)$$

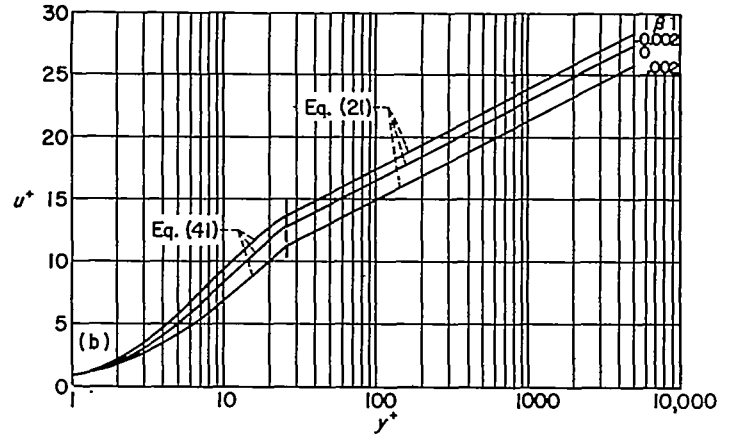
For variable viscosity, the expression for ϵ close to the wall (eq. (14)) can be written in dimensionless form as

$$\frac{\epsilon}{\mu_0/\rho_0} = n^2 u^+ y^+ \left(1 - e^{-\frac{n^2 u^+ y^+}{\mu/\mu_0}} \right) \quad (39)$$

For liquids, including water, oil, ethylene glycol, and sodium hydroxide, μ/μ_0 can usually be represented by $(t/t_0)^d$, if the liquid is not too near the freezing point. The exponent d varies from -1 to -4 , and the temperatures are measured in $^{\circ}F$. This differs from the case for gases where the temperatures were measured in $^{\circ}R$ (ref. 1). All the results up



(a) Temperature distribution.



(b) Velocity distribution.

FIGURE 8.—Generalized distribution for liquid with variable viscosity. Fully developed flow; Prandtl number, 10; $\mu/\mu_0 = (t/t_0)^{-1}$. (Vertical line is dividing line between eqs.)

to this point are independent of whether the temperatures are in $^{\circ}R$ or $^{\circ}F$. From the definitions of t^+ and β ,

$$\mu/\mu_0 = (1 - \beta t^+)^d \quad (40)$$

Substituting equations (39) and (40) into equations (37) and (38) and writing the result in integral form yield

$$u^+ = \int_0^{y^+} \frac{dy^+}{(1 - \beta t^+)^d + n^2 u^+ y^+ \left(1 - e^{-\frac{n^2 u^+ y^+}{(1 - \beta t^+)^d}} \right)} \quad (41)$$

and

$$t^+ = \int_0^{y^+} \frac{dy^+}{\frac{1}{Pr_0} + n^2 u^+ y^+ \left(1 - e^{-\frac{n^2 u^+ y^+}{(1 - \beta t^+)^d}} \right)} \quad (42)$$

Equations (41) and (42) can be solved simultaneously by iteration, that is, assumed values for u^+ , y^+ , and t^+ are substituted into the right side of the equations and new values of u^+ and t^+ are calculated by numerical integration. These new values are then substituted into the right side of the equations and the process is repeated until the values of u^+ and t^+ corresponding to each value of y^+ do not change appreciably. Equations (41) and (42) give the relations between u^+ , t^+ , and y^+ for various values of the heat-transfer parameter β and of Pr_0 for the region close to the wall.

In the region at a distance from the wall, the terms in the equations containing variable viscosity are neglected so that u^+ and t^+ are given by equations (21) and (22).

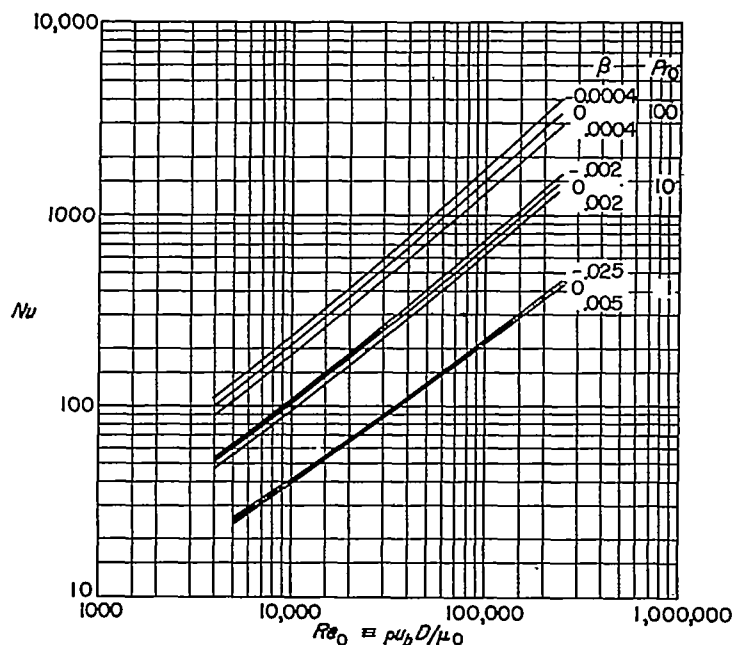


FIGURE 9.—Nusselt numbers against Reynolds numbers for various values of Prandtl number and heat-transfer parameter for liquids with variable viscosity. Fully developed flow; $\mu/\mu_0 = (t/t_0)^{-1}$.

Generalized temperature and velocity distributions for a Prandtl number at the wall of 10 and a d of -4 are shown for various values of the heat-transfer parameter β in figure 8. The value of y^+ at the intersection of the curves for flow close to and at a distance from the wall is taken as $y_1^+ = 26$, as in the case of constant viscosity. The effect of various assumptions for the variation of y_1^+ is investigated in reference 13 (fig. 13), in which it is concluded that this assumption should give accurate results. Positive values of β correspond to heat addition to the liquid, negative values to heat extraction. The values of t^+ at a given value of y^+ increase with increasing β , whereas the values of u^+ decrease. These opposite trends can be explained by examining the terms in the denominators of equations (41) and (42). The first term in the denominator of equation (41) (molecular) causes u^+ to decrease with increasing values of β ($d < 0$), whereas the second term (turbulent) causes u^+ to increase. The effect of the second term is somewhat smaller so that the net effect is a decrease, as shown in figure 8(b). In equation (42), however, the first term is independent of β and therefore the second term causes an increase in t^+ with increasing values of β . The opposite trends for heat transfer and friction in most of the succeeding curves can be attributed to the same cause.

The effect of the factor in parenthesis in equation (42), which is equal to F in equation (13), increases with increase in Prandtl number because of the steep temperature gradients at high Prandtl numbers in the region very close to the wall where F differs considerably from 1. The separation of the t^+ curves for various values of β (not shown) therefore increases as Prandtl number increases, the separation for a Prandtl number of 1 being very small.

For obtaining the relation between Nusselt number, Reynolds number, Prandtl number, and friction factor for variable viscosity, equations (23), (25), and (26) apply for variable properties as well as for constant properties if the

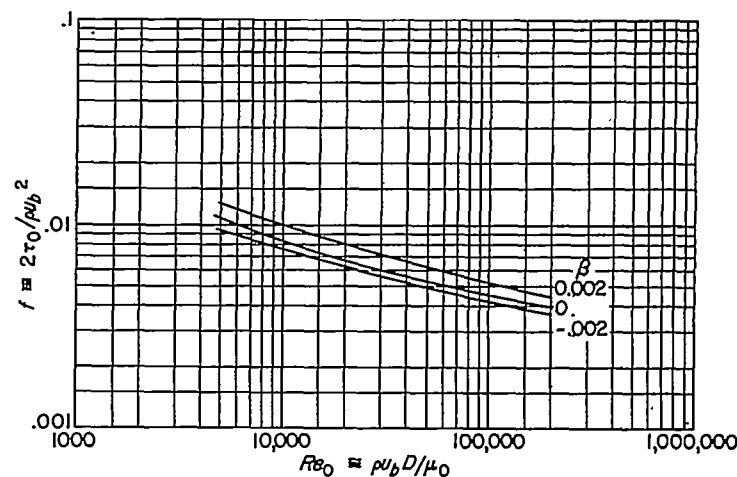


FIGURE 10.—Friction factors against Reynolds numbers for various values of heat-transfer parameter for liquids with variable viscosity. Fully developed flow; Prandtl number, 10; $\mu/\mu_0 = (t/t_0)^{-1}$.

viscosities in the Reynolds and Prandtl numbers are evaluated at the wall temperature. The friction factor f can be calculated from

$$f = 2/(u_b^+)^2 \quad (43)$$

Nusselt numbers and friction factors are plotted against Reynolds numbers in figures 9 and 10, respectively, with the viscosity in the Reynolds and Prandtl numbers evaluated at the wall temperature. The curves for cooling and heating are for values of μ_b/μ_0 on the order of 0.5 and 2, respectively. As in the case of temperature and velocity distributions, the trends with increasing values of β for the Nusselt numbers and friction factors are opposite. Also, as in the case of the temperature distributions, the separation of the Nusselt number curves with β increases as the Prandtl number increases, the separation being very small for a Prandtl number of 1. Thus, for a Prandtl number of 1 the reference temperature for evaluating the viscosity in order to eliminate the effects of variable viscosity is close to the wall temperature; the departure of the reference temperature from the wall temperature increases with Prandtl number. This is to be expected because, as mentioned previously in this section, the separation of the t^+ against y^+ curves with β increases with Prandtl number. In those curves all the properties are evaluated at the wall temperature.

The reference temperature for heat transfer in liquid with variable viscosity for a Prandtl number of 1 differs from that obtained for gases in reference 1, in which all the properties except the specific heat were considered variable. In reference 1, the reference temperature for gases was found to be close to the average of the wall and bulk temperatures rather than close to the wall temperature. In assigning a reference temperature, it is therefore important to consider what properties are variable.

Values of x for calculating the reference temperature t_x , where $t_x = x(t_0 - t_b) + t_b$, are given for heat transfer and friction in figure 11. The curves for $\beta = 0$ in figures 3 and 10 can be used for variable viscosity if the viscosities in the Reynolds and Prandtl numbers are evaluated at the reference temperatures given in figure 11 (Re_x and Pr_x). The values of x were computed for values of d ($\mu/\mu_0 = (t/t_0)^d$) of -1 and -4 and for

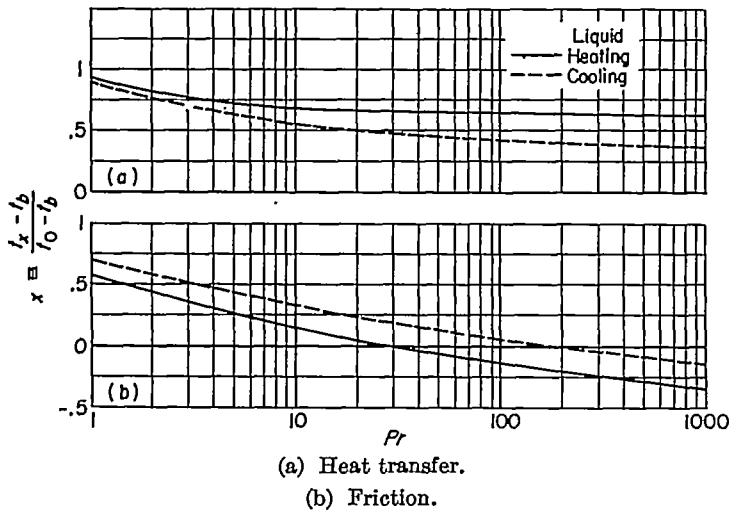


FIGURE 11.—Values of $x = (t_x - t_b)/(t_0 - t_b)$ against Prandtl number for evaluating viscosity in Prandtl and Reynolds numbers in figures 3 and 10 for liquids with variable viscosity. $\mu/\mu_0 = (t/t_0)^{-1}$ or $(t/t_0)^{-d}$; $\mu_b/\mu_0 \sim 0.5$ or 2 .

values of μ_b/μ_0 of about 0.5 and 2. The value of d had little effect on the curves, but different curves are obtained for heating and cooling of the liquid. In the case of heat transfer, the reference temperature does not depart greatly from that in the widely used Colburn equation (ref. 27), wherein the viscosity is evaluated at $t_{0.5}$ except at the lower Prandtl numbers. The values of x for friction are lower than those for heat transfer. Deviations from the curves in figure 11 might occur for very high viscosity ratios or for cases in which the viscosity variation with temperature could not be represented by a simple power function.

Turbulent heat transfer to gases with variable properties using present method of analysis.—If the present method of analysis is to be considered more general than the analysis in reference 1, it must be applicable to gases with variable properties as well as to liquids. When assumptions (1) and (2) in the section ANALYSIS FOR CONSTANT FLUID PROPERTIES are used, equations (4) and (5) become, for gases,

$$1 = \left(\frac{\mu}{\mu_0} + \frac{\rho}{\rho_0} \frac{\epsilon}{\mu_0/\rho_0} \right) \frac{du^+}{dy^+} \quad (44)$$

and

$$1 = \left(\frac{k}{k_0} \frac{1}{Pr_0} + \frac{\rho}{\rho_0} \frac{\epsilon}{\mu_0/\rho_0} \right) \frac{dt^+}{dy^+} \quad (45)$$

where c_p is assumed constant because its variation with temperature is slight compared with the variations of viscosity, thermal conductivity, and density. As in reference 1, it is assumed that $k/k_0 = \mu/\mu_0 = (t/t_0)^d$ and $\rho/\rho_0 = t_0/t$, where $d=0.68$ and the temperatures are measured in degrees Rankine. By substituting the expression for ϵ close to the wall (eq. (14)) and $t/t_0 = 1 - \beta t^+$, equations (44) and (45) can be written in integral form for the region close to the wall as

$$u^+ = \int_0^{y^+} \frac{dy^+}{(1 - \beta t^+)^d + \frac{n^2 u^+ y^+}{1 - \beta t^+} \left(1 - e^{-\frac{n^2 u^+ y^+}{(1 - \beta t^+)^{d+1}}} \right)} \quad (46)$$

$$t^+ = \int_0^{y^+} \frac{dy^+}{\frac{(1 - \beta t^+)^d}{Pr_0} + \frac{n^2 u^+ y^+}{1 - \beta t^+} \left(1 - e^{-\frac{n^2 u^+ y^+}{(1 - \beta t^+)^{d+1}}} \right)} \quad (47)$$

Equations (46) and (47) can be solved simultaneously by iteration as were equations (41) and (42).

In the region at a distance from the wall, the molecular shear-stress and heat-transfer terms in equations (44) and (45) are neglected and the expression for ϵ given in equation (15) is used. The integration is carried out in reference 1, in which it is found that

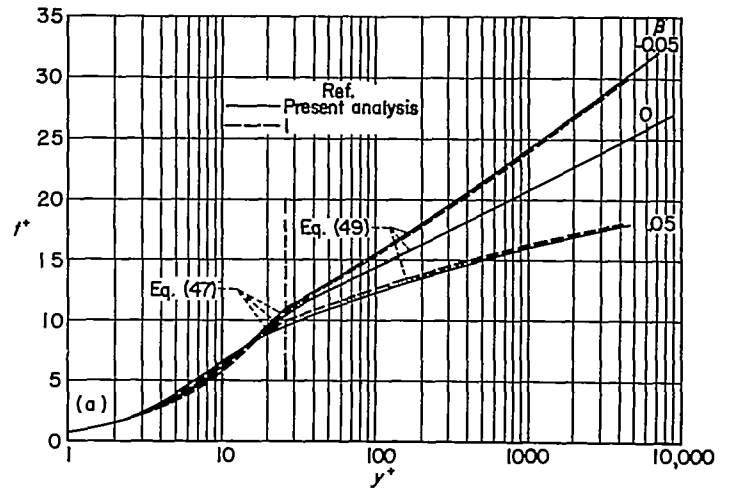
$$y^+ = \frac{y_1^+ e^{-\frac{2\kappa}{\beta} \sqrt{1 - \beta(u^+ - u_1^+ + t_1^+)}} \left[\frac{2\kappa}{\beta} \sqrt{1 - \beta(u^+ - u_1^+ + t_1^+)} + 1 \right]}{e^{-\frac{2\kappa}{\beta} \sqrt{1 - \beta t_1^+}} \left(\frac{2\kappa}{\beta} \sqrt{1 - \beta t_1^+} + 1 \right)} \quad (48)$$

and

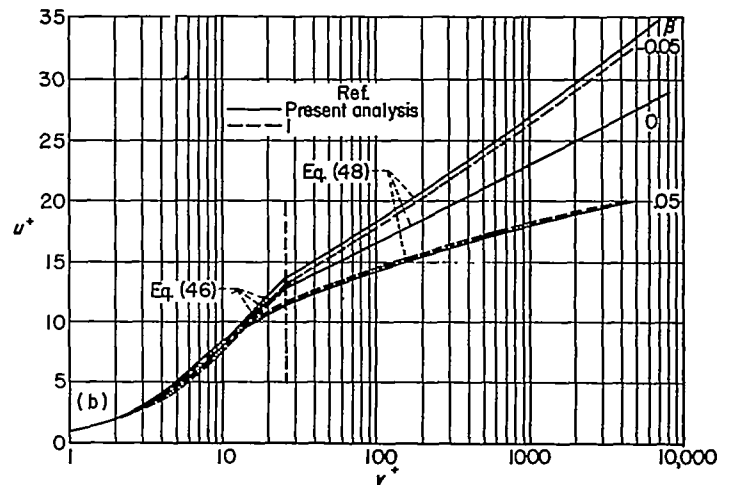
$$t^+ = t_1^+ + u^+ - u_1^+ \quad (49)$$

where $y_1^+ = 26$.

Generalized temperature and velocity distributions as calculated by the present analysis for a Prandtl number of 0.73 are plotted in figure 12. The distributions calculated in reference 1 are also included for comparison. The agreement between the two methods of analysis is satisfactory, so that the Nusselt numbers and the reference temperatures obtained from the present analysis should also agree with those given in reference 1.



(a) Temperature distribution.



(b) Velocity distribution.

FIGURE 12.—Comparison of generalized distributions for gases with variable properties. Prandtl number, 0.73. (Vertical line is dividing line between eqs.)

Laminar heat transfer to liquids with variable viscosity and uniform heat flux.—Laminar heat transfer to liquid metals with variable viscosity is investigated in reference 28. The results of that investigation should be applicable also to liquids with high Prandtl numbers if the value of d is on the order of -1.6 . The temperatures in the report are to be measured in $^{\circ}\text{F}$ ($\mu/\mu_0 = (t/t_0)^d$). It is found (ref. 28) that the results for fully developed laminar flow with constant heat flux can be represented closely by

$$Nu = \left(\frac{48}{11}\right) \left(\frac{\mu_0}{\mu}\right)^{0.14} \quad (50)$$

SUMMARY OF RESULTS

The following results were obtained from the analytical investigation of heat and mass transfer in smooth tubes at high Prandtl and Schmidt numbers:

1. By modifying the expression for eddy diffusivity from a previous analysis to account for the effect of kinematic viscosity in the region close to the wall, good agreement was obtained between predicted and experimental results for heat and mass transfer at Prandtl and Schmidt numbers between

0.5 and 3000. A simplified equation was obtained for very high Prandtl or Schmidt numbers.

2. The analysis indicated that, except at low Reynolds numbers, the entrance effect (local Nusselt number divided by fully developed Nusselt number) for heat or mass transfer decreases as Prandtl or Schmidt number increases.

3. The analysis indicated that the effects of variable viscosity on turbulent heat transfer and friction in liquids can be nearly eliminated in ordinary cases by evaluating the viscosities in the Reynolds and Prandtl numbers at reference temperatures which are functions of the Prandtl number. For the laminar case the results for liquid metals with variable viscosity given in a previous analysis should be applicable to liquids at high Prandtl numbers.

4. When the present method of analysis was applied to gases with variable properties, essentially the same results were obtained as are reported from analysis and experiments in a previous report.

LEWIS FLIGHT PROPULSION LABORATORY

NATIONAL ADVISORY COMMITTEE FOR AERONAUTICS

CLEVELAND, OHIO, February 17, 1954

APPENDIX

SYMBOLS

The following symbols are used in this report:

C	concentration of diffusing substance, (lb) (sec ³)/ft ⁴
C_b	bulk concentration of diffusing substance (lb) (sec ³)/ft ⁴
C_δ	concentration of diffusing substance at $y=\delta$, (lb) (sec ³)/ft ⁴
C_0	concentration of diffusing substance at wall, (lb) (sec ³)/ft ⁴
c	exponent
c_p	specific heat of fluid at constant pressure, Btu/(lb)($^{\circ}\text{F}$)
$c_{p,0}$	specific heat of fluid at constant pressure at wall, Btu/(lb)($^{\circ}\text{F}$)
D	inside diameter of tube, ft
d	exponent, value of which depends on variation of viscosity of fluid with temperature
F	function of $\epsilon/(\mu/\rho)$
g	conversion constant, 32.2 ft/sec ²
h	local heat-transfer coefficient, $q_0/t_0 - t_b$, Btu/(sec) (sq ft) ($^{\circ}\text{F}$)
h'	local mass-transfer coefficient, $m_0/(C_0 - C_b)$, ft/sec
h_{av}	average heat-transfer coefficient, $q_0/(t_0 - t_b)_{av}$
h'_{av}	average mass-transfer coefficient, $m_0/(C_0 - C_b)_{av}$
k	thermal conductivity of fluid, Btu/(sec) (sq ft) ($^{\circ}\text{F}/\text{ft}$)
k_0	thermal conductivity of fluid evaluated at t_0 , Btu/(sec) (sq ft) ($^{\circ}\text{F}/\text{ft}$)
m	rate of mass transfer toward tube center per unit area, (lb) (sec)/cu ft
m_0	rate of mass transfer toward tube center per unit area at wall, (lb) (sec)/cu ft
n	constant

q	rate of heat transfer toward tube center per unit area, Btu/(sec) (sq ft)
q_0	rate of heat transfer at inside wall toward tube center per unit area, Btu/(sec) (sq ft)
r_0	inside tube radius, ft
t	temperature, $^{\circ}\text{F}$ for liquids or $^{\circ}\text{R}$ for gases
t_b	bulk static temperature of fluid at cross section of tube, $^{\circ}\text{F}$
t_x	reference temperature for local Reynolds and Prandtl numbers, $x(t_0 - t_b) + t_b$, $^{\circ}\text{F}$
t_δ	temperature of fluid outside thermal boundary layer, $^{\circ}\text{F}$
t_0	wall temperature, $^{\circ}\text{F}$ for liquids or $^{\circ}\text{R}$ for gases
$(t_0 - t_b)_{av}$	average difference between wall and bulk temperature, $^{\circ}\text{F}$
u	time-average velocity parallel to axis of tube, ft/sec
u_b	bulk velocity at cross section of tube, ft/sec
X	distance from point at which heat or mass transfer begins, ft
x	number used in evaluating arbitrary temperature in tube t_x
y	distance from wall, ft
δ_h	thermal or diffusion boundary-layer thickness, ft
ϵ	coefficient of eddy diffusivity for momentum, sq ft/sec
ϵ'	expression for eddy diffusivity which neglects effect of μ/ρ , sq ft/sec
ϵ_h	coefficient of eddy diffusivity for heat or mass, sq ft/sec
κ	Kármán constant
λ	molecular diffusivity, sq ft/sec

λ_0	molecular diffusivity at wall, sq ft/sec
μ	absolute viscosity of fluid, (lb) (sec)/sq ft
μ_b	absolute viscosity of fluid evaluated at t_b , (lb) (sec)/sq ft
μ_x	absolute viscosity of fluid evaluated at t_x , (lb) (sec)/sq ft
μ_0	absolute viscosity of fluid evaluated at t_0 , (lb) (sec)/sq ft
ρ	mass density of fluid, (lb) (sec ²)/ft ⁴
ρ_0	mass density of fluid evaluated at t_0 , (lb)(sec ²)/ft ⁴
τ	shear stress in fluid, lb/sq ft
τ_0	shear stress in fluid at wall, lb/sq ft
Dimensionless groups:	

C^+	concentration parameter, $\frac{(C_0 - C)\sqrt{\tau_0/\rho_0}}{m_0}$
C_b^+	bulk concentration parameter, $\frac{(C_0 - C_b)\sqrt{\tau_0/\rho_0}}{m_0}$
C_δ^+	value of C^+ at δ_n^+ , $\frac{(C_0 - C_\delta)\sqrt{\tau_0/\rho_0}}{m_0}$
C_1^+	value of C^+ at y_1^+
f	friction factor, $2\tau_0/\rho u_b^2$
Nu	Nusselt number for heat transfer, hD/k
Nu'	Nusselt number for mass transfer, $h'D/\lambda$
Nu_{av}	average Nusselt number for heat transfer, $h_{av}D/k$
Nu_{av}'	average Nusselt number for mass transfer, $h_{av}'D/\lambda$
Nu_d	fully developed Nusselt number for heat transfer
Nu_d'	fully developed Nusselt number for mass transfer
Pe	Peclet number, $\rho u_b D c_p g/k$
Pr	Prandtl number, $c_p g \mu/k$
Pr_0	Prandtl number with properties evaluated at t_0

Re	Reynolds number, $\rho u_b D/\mu$
Re_x	Reynolds number with viscosity evaluated at t_x , $\rho u_b D/\mu_x$
Re_0	Reynolds number with viscosity evaluated at t_0 , $\rho u_b D/\mu_0$
r_0^+	tube radius parameter, $\frac{\sqrt{\tau_0/\rho_0}}{\mu_0/\rho_0} r_0$
Sc	Schmidt number, $\mu/(\rho\lambda)$
Sc_0	Schmidt number at wall, $\mu_0/\rho_0\lambda_0$
St	Stanton number for heat transfer, $h/\rho g u_b c_p$
St'	Stanton number for mass transfer, h'/u_b
t^+	temperature parameter, $\frac{(t_0 - t)c_p g \tau_0}{q_0 \sqrt{\tau_0/\rho_0}} = \frac{1 - t/t_0}{\beta}$
t_b^+	bulk-temperature parameter, $\frac{1}{\beta} \left(1 - \frac{t_b}{t_0}\right)$
t_δ^+	$\frac{1}{\beta} \left(1 - \frac{t_\delta}{t_0}\right)$
t_1^+	value of t^+ at y_1^+
u^+	velocity parameter, $u/\sqrt{\tau_0/\rho_0}$
u_b^+	bulk-velocity parameter, $u_b/\sqrt{\tau_0/\rho_0}$
u_1^+	value of u^+ at y_1^+
y^+	wall distance parameter, $\frac{\sqrt{\tau_0/\rho_0}}{\mu_0/\rho_0} y$
y_1^+	value of y^+ at intersection of curves for flow close to wall and at a distance from wall
α	ratio of eddy diffusivities, ϵ_h/ϵ
β	heat-transfer parameter, $q_0 \sqrt{\tau_0/\rho_0}/(c_p g \tau_0 t_0)$
δ_n^+	dimensionless thermal or diffusion boundary-layer thickness, $\frac{\sqrt{\tau_0/\rho_0}}{\mu_0/\rho_0} \delta_n$

REFERENCES

- Deissler, R. G., and Eian, C. S.: Analytical and Experimental Investigation of Fully Developed Turbulent Flow of Air in a Smooth Tube with Heat Transfer with Variable Fluid Properties. NACA TN 2629, 1952.
- von Kármán, Th.: The Analogy Between Fluid Friction and Heat Transfer. Trans. A.S.M.E., vol. 61, no. 8, Nov. 1939, pp. 705-710.
- Summerfield, Martin: Recent Developments in Convective Heat Transfer with Special Reference to High-Temperature Combustion Chambers. Heat Transfer Symposium, Eng. Res. Inst., Univ. Mich., 1953, pp. 151-171.
- Murphree, E. V.: Relation Between Heat Transfer and Fluid Friction. Ind. and Eng. Chem., vol. 24, no. 7, July 1932, pp. 726-736.
- Lin, C. S., Moulton, R. W., and Putnam, G. L.: Mass Transfer Between Solid Wall and Fluid Streams. Ind. and Eng. Chem., vol. 45, no. 3, Mar. 1953, pp. 636-640.
- Sherwood, Thomas K.: Heat Transfer, Mass Transfer, and Fluid Friction-Relationships in Turbulent Flow. Ind. and Eng. Chem., vol. 42, no. 10, Oct. 1950, pp. 2077-2084.
- Martinelli, R. C.: Heat Transfer to Molten Metals. Trans. A.S.M.E., vol. 69, no. 8, Nov. 1947, pp. 947-959.
- Deissler, Robert G.: Analytical and Experimental Investigation of Adiabatic Turbulent Flow in Smooth Tubes. NACA TN 2138, 1950.
- Deissler, Robert G.: Analysis of Fully Developed Turbulent Heat Transfer at Low Peclet Numbers in Smooth Tubes with Application to Liquid Metals. NACA RM E52F05, 1952.
- Deissler, Robert G.: Analysis of Turbulent Heat Transfer and Flow in the Entrance Regions of Smooth Passages. NACA TN 3016, 1953.
- Laufer, John: The Structure of Turbulence in Fully Developed Pipe Flow. NACA TN 2954, 1953.
- Deissler, Robert G., and Taylor, Maynard F.: Analysis of Heat Transfer and Fluid Friction for Fully Developed Turbulent Flow of Supercritical Water with Variable Fluid Properties in a Smooth Tube. NACA RM E53B17, 1953.
- Deissler, R. G.: Heat Transfer and Fluid Friction for Fully Developed Turbulent Flow of Air and Supercritical Water with Variable Fluid Properties. Trans. A.S.M.E., vol. 76, no. 1, Jan. 1954, pp. 73-85.
- Bernardo, Everett, and Eian, Carroll S.: Heat Transfer Tests of Aqueous Ethylene Glycol Solutions in an Electrically Heated Tube. NACA WR E-136, 1945. (Supersedes NACA ARR E5F07.)
- Kaufman, Samuel J., and Isely, Francis D.: Preliminary Investigation of Heat Transfer to Water Flowing in an Electrically Heated Inconel Tube. NACA RM E50G31, 1950.
- Eagle, A. E., and Ferguson, R. M.: On the Coefficient of Heat Transfer from the Internal Surface of Tube Walls. Proc. Roy. Soc. (London), ser. A, vol. 127, 1930, pp. 540-566.
- Kreith, F., and Summerfield, M.: Pressure Drop and Convective Heat Transfer with Surface Boiling at High Heat Flux; Data for Aniline and n-Butyl Alcohol. Trans. A.S.M.E., vol. 72, no. 6, Aug. 1950, pp. 869-878; discussion, pp. 878-879.
- Grele, Milton D., and Gedeon, Louis: Forced-Convection Heat-Transfer Characteristics of Molten Sodium Hydroxide. NACA RM E53L09, 1953.
- Hoffman, H. W.: Turbulent Forced Convection Heat Transfer in Circular Tubes Containing Molten Sodium Hydroxide. ORNL-1370, Reactor Exp. Eng. Div., Oak Ridge Nat. Lab., Oak Ridge (Tenn.), Oct. 3, 1952. (Contract No. W-7405, eng. 26.)

20. Barnet, Walter I., and Kobe, Kenneth A.: Heat and Vapor Transfer in a Wetted-Wall Tower. *Ind. and Eng. Chem.*, vol. 33, no. 4, Apr. 1941, pp. 436-442.
21. Chilton, T. H., and Colburn, A. P.: Mass Transfer (Absorption) Coefficients. *Ind. and Eng. Chem.*, vol. 26, no. 11, Nov. 1934, pp. 1183-1187.
22. Jackson, M. L., and Ceaglske, N. H.: Distillation, Vaporization, and Gas Absorption in a Wetted-Wall Column. *Ind. and Eng. Chem.*, vol. 42, no. 6, June 1950, pp. 1188-1198.
23. Bonilla, Charles F.: Mass Transfer in Liquid Metal and Fused Salt Systems. NYO-3086, First Quarterly Prog. Rep., U. S. Atomic Energy Comm., Tech. Information Service, Oak Ridge (Tenn.), Sept. 1, 1951. (Contract No. AT (30-1)-1100.)
24. Linton, W. H., Jr., and Sherwood, T. K.: Mass Transfer from Solid Shapes to Water in Streamline and Turbulent Flow. *Chem. Eng. Prog.*, vol. 46, no. 5, May 1950, pp. 258-264.
25. Lin, C. S., Denton, E. B., Gaskill, H. S., and Putnam, G. L.: Diffusion-Controlled Electrode Reactions. *Ind. and Eng. Chem.*, vol. 43, no. 9, Sept. 1951, pp. 2136-2143.
26. Poppendiek, H. F., and Palmer, L. D.: Forced Convection Heat Transfer in Thermal Entrance Regions, Pt. II. ORNL 914, Metallurgy and Ceramics, Reactor Exp. Eng. Div., Oak Ridge Nat. Lab., Oak Ridge (Tenn.), May 26, 1952. (Contract No. W-7405, eng. 26.)
27. McAdams, William H.: Heat Transmission. Second ed., McGraw-Hill Book Co., Inc., 1942, p. 168.
28. Deissler, Robert G.: Analytical Investigation of Fully Developed Laminar Flow in Tubes with Heat Transfer with Fluid Properties Variable Along the Radius. NACA TN 2410, 1951.